EPJ Web of Conferences **182**, 02002 (2018) https://doi.org/10.1051/epjconf/201818202002
ICNFP 2017

Search for $K^+ \to \pi^+ \nu\bar{\nu}$ at NA62

Riccardo Aliberti[1,a] on behalf of the NA62 collaboration[b]

[1]*Johannes Gutenberg University, Mainz, Germany*

Abstract. Flavour physics is one of the most powerful fields for the search of new physics beyond the Standard Model. The kaon sector with the rare decay $K^+ \to \pi^+ \nu\bar{\nu}$ provides one of the cleanest and most promising channels. NA62, a fixed target experiment at the CERN SPS, aims to measure $BR(K^+ \to \pi^+ \nu\bar{\nu})$ with 10% precision to test the Standard Model validity up to an energy scale of hundreds of TeV. NA62 had dedicated data taking for the $K^+ \to \pi^+ \nu\bar{\nu}$ measurement in 2016 and 2017 and will continue in 2018. Here preliminary results on a fraction of 2016 dataset are presented. The analysis of the complete 2016 data sample is expected to achieve the SM sensitivity.

1 Introduction

The present status of particle physics has many open questions that do not have answer inside the framework of the Standard Model (SM). The very different mass scales from neutrinos up to the top quark, dark matter and baryon/anti-baryon asymmetry are just few examples of missing pieces in the puzzle of describing nature in a fully consistent model. Direct searches of new physics at the LHC have not provided, until now, any evidence of exotic particles or processes up to few TeV.
Indirect searches provide an effective tool to explore mass scales which are completely unreachable by

[a]e-mail: riccardo.aliberti@cern.ch

[b]R. Aliberti, F. Ambrosino, R. Ammendola, B. Angelucci, A. Antonelli, G. Anzivino, R. Arcidiacono, M. Barbanera, A. Biagioni, L. Bician, C. Biino, A. Bizzeti, T. Blazek, B. Bloch-Devaux, V. Bonaiuto, M. Boretto, M. Bragadireanu, D. Britton, F. Brizioli, M.B. Brunetti, D. Bryman, F. Bucci, T. Capussela, A. Ceccucci, P. Cenci, V. Cerny, C. Cerri, B. Checcucci, A. Conovaloff, P. Cooper, E. Cortina Gil, M. Corvino, F. Costantini, A. Cotta Ramusino, D. Coward, G. D'Agostini, J. Dainton, P. Dalpiaz, H. Danielsson, N. De Simone, D. Di Filippo, L. Di Lella, N. Doble, B. Dobrich, F. Duval, V. Duk, J. Engelfried, T. Enik, N. Estrada-Tristan, V. Falaleev, R. Fantechi, V. Fascianelli, L. Federici, S. Fedotov, A. Filippi, M. Fiorini, J. Fry, J. Fu, A. Fucci, L. Fulton, E. Gamberini, L. Gatignon, G. Georgiev, S. Ghinescu, A. Gianoli, M. Giorgi, S. Giudici, F. Gonnella, E. Goudzovski, C. Graham, R. Guida, E. Gushchin, F. Hahn, H. Heath, T. Husek, O. Hutanu, D. Hutchcroft, L. Iacobuzio, E. Iacopini, E. Imbergamo, B. Jenninger, K. Kampf, V. Kekelidze, S. Kholodenko, G. Khoriauli, A. Khotyantsev, A. Kleimenova, A. Korotkova, M. Koval, V. Kozhuharov, Z. Kucerova, Y. Kudenko, J. Kunze, V. Kurochka, V.Kurshetsov, G. Lanfranchi, G. Lamanna, G. Latino, P. Laycock, C. Lazzeroni, M. Lenti, G. Lehmann Miotto, E. Leonardi, P. Lichard, L. Litov, R. Lollini, D. Lomidze, A. Lonardo, P. Lubrano, M. Lupi, N. Lurkin, D. Madigozhin, I. Mannelli, G. Mannocchi, A. Mapelli, F. Marchetto, R. Marchevski, S. Martellotti, P. Massarotti, K. Massri, E. Maurice, M. Medvedeva, A. Mefodev, E. Menichetti, E. Migliore, E. Minucci, M. Mirra, M. Misheva, N. Molokanova, M. Moulson, S. Movchan, M. Napolitano, I. Neri, F. Newson, A. Norton, M. Noy, T. Numao, V. Obraztsov, A. Ostankov, S. Padolski, R. Page, V. Palladino, C. Parkinson, E. Pedreschi, M. Pepe, M. Perrin-Terrin, L. Peruzzo, P. Petrov, F. Petrucci, R. Piandani, M. Piccini, J. Pinzino, I. Polenkevich, L. Pontisso, Yu. Potrebenikov, D. Protopopescu, M. Raggi, A. Romano, P. Rubin, G. Ruggiero, V. Ryjov, A. Salamon, C. Santoni, G. Saracino, F. Sargeni, V. Semenov, A. Sergi, A. Shaikhiev, S. Shkarovskiy, D. Soldi, V. Sougonyaev, M. Sozzi, T. Spadaro, F. Spinella, A. Sturgess, J. Swallow, S. Trilov, P. Valente, B. Velghe, S. Venditti, P. Vicini, R. Volpe, M. Vormstein, H. Wahl, R. Wanke, B. Wrona, O. Yushchenko, M. Zamkovsky, A. Zinchenko.

the current accelerator machines. As an example, in 1970 the charm quark was predicted by Glashow, Iliopoulos and Maiani following the experimental observation that $\Delta S = 2$ transitions were strongly disfavoured respect to $\Delta S = 1$ processes [1]. In this view SM predictions of several processes are under investigation. The kaon decay $K \to \pi\nu\bar{\nu}$ provide one of the most interesting transitions in both the neutral ($K_L \to \pi^0\nu\bar{\nu}$) and the charged ($K^+ \to \pi^+\nu\bar{\nu}$) sector.
The decays take place through Flavour Changing Neutral Current processes with quadratic GIM suppression, resulting in SM branching ratios of the order of 10^{-11} [2].

$$BR(K_L \to \pi^0\nu\bar{\nu}) = (3.4 \pm 0.6) \times 10^{-11}$$
$$BR(K^+ \to \pi^+\nu\bar{\nu}) = (8.4 \pm 1.0) \times 10^{-11}$$

These processes are theoretically very clean, since hadronic contribution uncertainties can be estimated to a few percent by extrapolating the $K \to \pi$ transition form factor from the leading semileptonic kaon decays (K_{l3}, with $l = e, \mu$) via an isospin rotation [3]. Many expansions of the SM predict significant contributions to the branching ratio of this process by new particles inside the Feynman loop diagrams (figure 1). The $K \to \pi\nu\bar{\nu}$ decay is therefore sensitive to new physics up to energy scales of several hundreds of TeV [4]. A precise measurement of this decay in both charged and neutral sectors represents a severe check of the Standard Model in still unexplored energy scales.

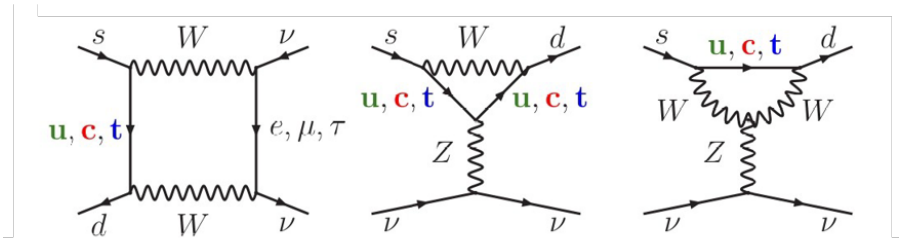

Figure 1. Feynman diagrams of the $K^+ \to \pi^+\nu\bar{\nu}$ decay.

The experimental measurement of $K \to \pi\nu\bar{\nu}$, however, presents significant difficulties due to the weak signature of the decay and to the very tiny branching ratio. The current results are $BR(K_L \to \pi^0\nu\bar{\nu}) < 2.6 \times 10^{-8}$ at 90% CL and $BR(K^+ \to \pi^+\nu\bar{\nu}) = \left(17.3^{+11.5}_{-10.5}\right) \times 10^{-11}$ respectively from the E391a [5] and the E949 [6] collaborations.
The KOTO [7] experiment currently running at J-PARC in Japan aims to observe few $K_L \to \pi^0\nu\bar{\nu}$ SM events by 2021 [8]. Meanwhile at CERN the NA62 experiment aims to measure the $K^+ \to \pi^+\nu\bar{\nu}$ branching ratio with 10% precision. First preliminary results are presented in the following.

2 The NA62 Experiment

NA62 is a fixed target experiment located in the North Area of CERN that aims to measure $BR(K^+ \to \pi^+\nu\bar{\nu})$ with the decay-in-flight technique. The experiment carries on the long tradition of kaon experiments at the CERN SPS leading to fundamental knowledge of the weak interaction with the measurement of direct CP violation by NA31 and NA48.
The measurement of $K^+ \to \pi^+\nu\bar{\nu}$ determines the design of the apparatus. The very tiny branching fraction of the process imposes a high intensity beam that allows to collect about 5×10^{12} kaon decays per year.

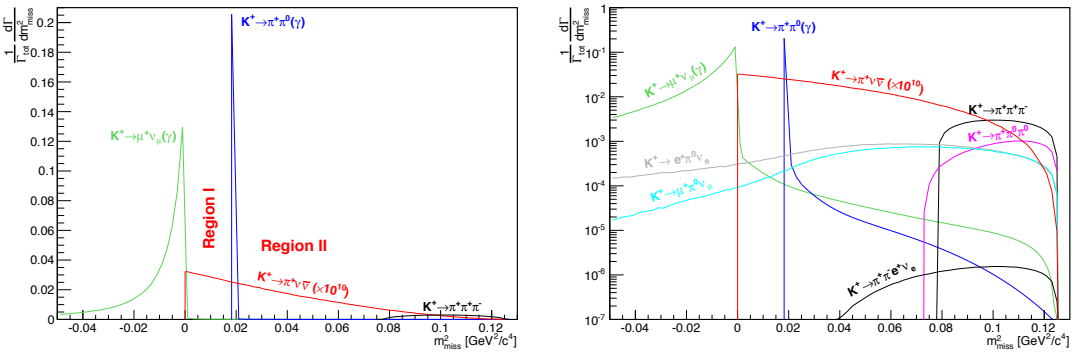

Figure 2. Squared missing mass variable distribution for the main kaon decays in linear (left) and logarithmic (right) scale.

The signature of the $K^+ \to \pi^+ \nu\bar{\nu}$ decay can be summarized with the presence of a kaon in the initial state and of a charged pion in the final state, while the neutrinos escape undetected.
The main kinematic variable in the analysis is the invariant squared missing mass $m^2_{miss} = \left(P^2_K - P^2_\pi\right)$, where P_k and P_π are the measured kaon and pion 4-momenta. It provides a kinematical discrimination between the main kaon decays. Two different signal regions exist as shown in figure 2: Region I (R1) is defined between the $K^+ \to \mu^+\nu_\mu$ ($K_{\mu 2}$) and the $K^+ \to \pi^+\pi^0$ ($K_{2\pi}$) decay distributions, while Region II (R2) extends up to the $K \to 3\pi$ region. A precise kinematic reconstruction of the event is therefore a crucial requirement for the $K^+ \to \pi^+ \nu\bar{\nu}$ analysis.
A very efficient particle identification and an hermetic photon detection are required in order to suppress the kinematic tails of the $K_{\mu 2}$ and $K_{2\pi}$ decays. The selection of a pion momentum in the range of [15, 35] GeV/c allows to constrain the energy of the π^0s from $K^+ \to \pi^+\pi^0$ to be above 40 GeV and to reach the required photon veto efficiency.
The high beam particle rate required for the measurement represents a dangerous background source due to accidental overlaps of events. A sub-nanosecond time resolution in the matching between beam particles and decay products is therefore indispensable to minimize the mismatching probability.
A scheme of the NA62 detector is presented in figure 3. It consists of two different regions: upstream, devoted to the identification and measurement of the beam particles, and downstream, characterizing the decay products. A comprehensive description of the NA62 beam and detector can be found in ref. [9].

The 400 GeV/c proton beam from the SPS impinges on a beryllium target, generating a secondary hadron beam where the positive component at 75 GeV/c is selected and collimated in a 100 m long beam line. The final beam has a particle rate of 750 MHz out of which only 6% is due to kaons, resulting in 5 MHz of K^+ decays inside the fiducial volume.
The kaon component of the beam is identified and timestamped by a differential cherenkov counter (KTAG). Three stations of silicon pixel detectors compose the beam tracker (GTK), performing momentum and direction measurement for each particle. Inelastic scattering of kaons on last station of the GTK detector can result in a pion mimicking the $K^+ \to \pi^+ \nu\bar{\nu}$ signal. In order to veto these dangerous events scintillating anti-counters (CHANTI) are installed around the end of last collimator. The fiducial region is 50 meters long, starting 10 m after the last station of the GTK, in order to suppress background from residual interactions in this detector, and ends 15 m before the spectrometer,

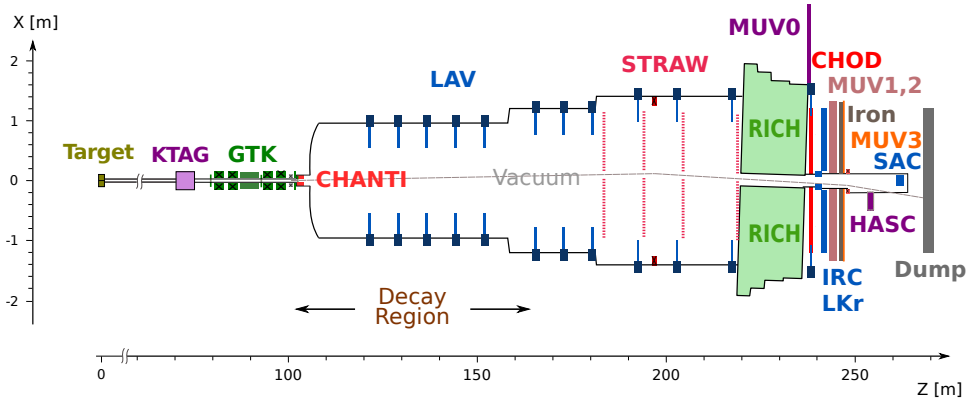

Figure 3. The NA62 detector.

imposed by acceptance requirements to veto kaon decays into three charged pions. The spectrometer (STRAW), composed of four chambers of straw tubes, provides a precise measurement of momenta and directions of the kaon decay products. In order to maximize the kinematic measurement precision, the complete decay volume, from the target to the last station of the STRAW spectrometer, is kept in vacuum (10^{-6} mbar).
A ring imaging cherenkov detector (RICH) identifies and timestamps the downstream tracks with better than 100 ps time resolution. The electromagnetic (LKr) and hadronic (MUV1,2) calorimeters refine the particle identification and a fast muon veto (MUV3), placed behind a 80 cm thick iron wall, provides the muon rejection at trigger level. Two plastic scintillator hodoscopes (CHODs) provide timing information and contribute to the trigger.
Twelve stations of large angle photon anti-counters (LAV) are placed between the GTK and the LKr calorimeter in order to veto events with photons escaping the apparatus at large angle ([8, 50] mrad). The electromagnetic calorimeter performs the detection of photons emitted at intermediate angles ([1, 8] mrad) and two small shashlik calorimeters (IRC and SAC), in front of the LKr and at the end of the beam pipe, extend the coverage down to 0 mrad.
Data collection is performed by using two independent trigger chains: one (Physics Trigger) selects candidate events for the $K^+ \to \pi^+\nu\bar{\nu}$ measurement while the other (Control Trigger) provides a minimally biased sample used, for example, to perform trigger efficiency and normalisation studies.

In 2015 and 2016 NA62 performed the full commissioning of the detector. Low intensity data collected in 2015 with a minimum-bias trigger allowed to study detector performances and to perform physics analysis. In 2016 beam intensity was gradually rose and between September and November a first high quality dataset for the $K^+ \to \pi^+\nu\bar{\nu}$ analysis was collected at around 40% of the nominal beam intensity. A 6 months long run dedicated to $K^+ \to \pi^+\nu\bar{\nu}$ data taking was performed in 2017 and another one is scheduled for 2018.
In the following preliminary results based on 5% of the data collected in 2016, corresponding to 2.3×10^{10} kaon decays, are presented.

3 Analysis

The signature of the $K^+ \to \pi^+\nu\bar{\nu}$ decay is the presence of a kaon in the initial state and a pion in the final state. In this context the first step of the analysis consists in the selection of events with a single track in the spectrometer, matching a beam track reconstructed in the GTK and identified as a kaon by the KTAG. The reconstructed vertex is then required to be inside the fiducial region. Figure 4 shows the distribution of the Squared Missing Mass, $m^2_{miss} = \left(P^2_K - P^2_\pi\right)$, as a function of the pion momentum on a minimum-bias sample (Control Trigger) before and after kaon identification. The main kaon decays to be suppressed are clearly visible in these plots: the central horizontal line are $K^+ \to \pi^+\pi^0$ ($K_{2\pi}$) events, the lower rising band is from $K^+ \to \mu^+\nu_\mu$ ($K_{\mu 2}$) and on the top of the distribution $K \to 3\pi$ ($K_{3\pi}$) decays can be found. Semi-leptonic kaon decays, $K^+ \to \pi^0 l^+ \nu_l$ (K_{l3} with $l = e, \mu$), fill the missing mass region between $K_{2\pi}$ and $K_{3\pi}$. In the left picture it is possible to observe two additional characteristic features: elastic scattering of beam particles on the last station of the beam tracker results in a band around 75 GeV/c, and decays of beam pions into muons generate a broad distribution below the $K_{\mu 2}$ curve. The red boxes on the right plot indicate the signal regions of the analysis.

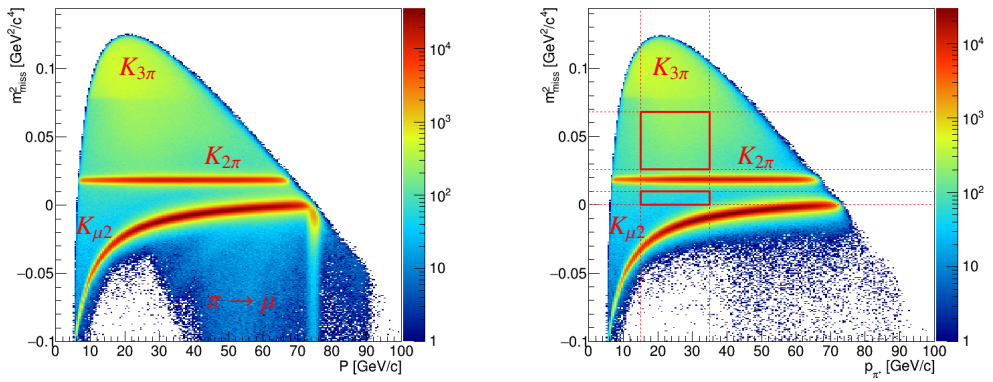

Figure 4. Squared Missing Mass as a function of the pion momentum before (left) and after (right) kaon identification. On the right plot two red boxes show the signal regions of the $K^+ \to \pi^+\nu\bar{\nu}$ analysis.

3.1 Kinematic Rejection

A precise knowledge of the kinematic variables is essential for the $K^+ \to \pi^+\nu\bar{\nu}$ measurement: non-gaussian tales in the missing mass distributions of $K_{2\pi}$, $K_{\mu 2}$ and $K_{3\pi}$ from resolution effects and erroneous matching between upstream and downstream tracks represent dangerous sources of background.

Kaon-Pion mismatching

The association between beam kaons and decay pions is performed with a linear discriminant exploiting the time differences and the closest distance of approach of the two tracks. A kaon identification

by the KTAG is required within 2 ns from the RICH time. A selection of $K^+ \to \pi^+\pi^+\pi^-$, performed using only information from the downstream detectors, is used to determine the parameters of the discriminant and the resulting performances. The probability to wrongly associate a kaon track with a downstream track is below 2% at 40% of the nominal beam intensity and with an efficiency of 75% for the correct matching.

Kinematic tails

Contribution of mismatching and of wrongly measured pion momentum to the non-gaussian tail of the squared missing mass can be mitigated by cross-checking m^2_{miss} with independent sources. The reference squared missing mass estimation is determined by using the momenta measured by the GTK and the STRAW, but redundant information can be obtained by the nominal beam parameters and by the reconstructed RICH ring. Therefore the squared missing mass is estimated by considering three different combinations of kaon and pion momentum measurements: GTK-STRAW, Nominal beam-STRAW, and GTK-RICH.
A selection of $K^+ \to \pi^+\pi^0$ events based on particle identification and a fully reconstructed π^0 is used to estimate the contribution of kinematic tails of $K_{2\pi}$ inside the signal regions. Figure 5 shows the distributions of the three missing mass values. The fraction of events inside the signal regions is 1.6×10^{-4} in R1 and 4.2×10^{-4} in R2.

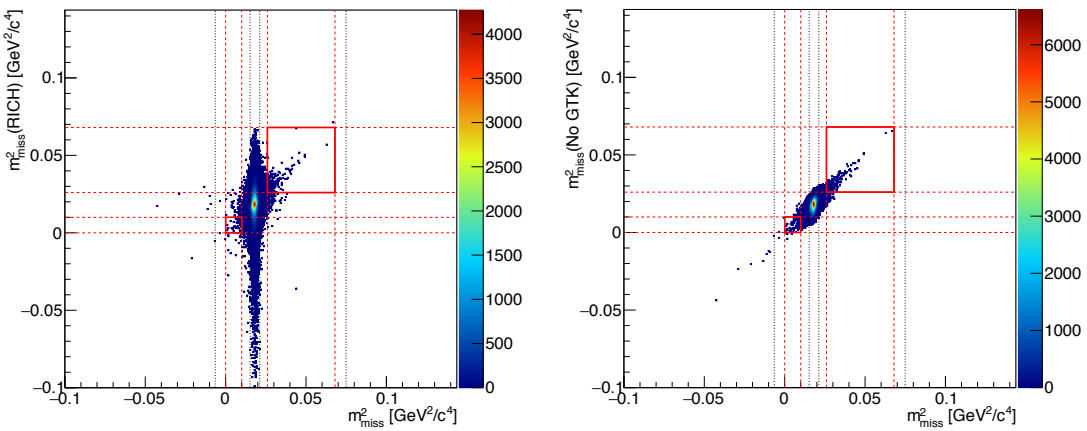

Figure 5. Squared missing mass distributions for $K_{2\pi}$ events. Measured, on the left, with GTK-STRAW on the X-axis and with GTK-RICH on the Y-axis. On the right computed from the GTK-STRAW on the X-axis and the nominal kaon momentum-STRAW on the Y-axis.

Similarly a $K_{\mu 2}$ sample, based on photon veto and particle identification, is selected to evaluate the kinematic tails of these events. In this case the RICH was not applied in neither particle identification nor missing mass computation because mass and momentum measurements from this detector are fully correlated. The contribution of the $K^+ \to \mu^+\nu_\mu$ tails to the signal regions is estimated as $(2.5 \pm 0.1) \times 10^{-4}$ in R1 and $(0.4 \pm 0.1) \times 10^{-4}$ in R2.

The $K \to 3\pi$ contribution to the signal regions is evaluated to 10^{-4} using MC. A method to more precise estimate by using larger MC sample together with data is currently under study.

3.2 Particle Identification

The leading kaon decay, $K^+ \to \mu^+\nu_\mu$, have a branching ratio of (63.56 ± 0.11) %[10]. In order to keep the background contribution to $K^+ \to \pi^+\nu\bar{\nu}$ measurement at the level of 10%, muon-pion separation of the order of 10^7 is needed. This result is achieved by combining the information from several detectors: RICH, MUV3, and Calorimeters.
The RICH pion identification follows two independent paths: a likelihood analysis and a standalone ring reconstruction. In the first method, starting from the track informations, the expected ring is evaluated for various mass hypotheses and compared with the hits recorded in order to obtain a likelihood value for each tested mass value. The second procedure applies a standalone ring reconstruction in the assumption of a single track event. The reconstructed ring informations are then combined with the spectrometer momentum measurement to estimate the mass of the crossing particle. Analogously, by imposing the mass, the ring radius provides a measurement of the track momentum.
The informations from the electromagnetic and hadronic calorimeters are combined into a multivariate analysis (MVA) to perform the particle identification. The MVA is based on a Boosted Decision Tree, with 13 input variables parametrizing the lateral and longitudinal shower profiles in the different detector modules and the ratio between reconstructed energy and track momentum. In addiction, all events having an in time hit in the MUV3 detector are considered not to be a pion.
The performance of the muon-pion separation is evaluated by a strictly kinematic selection of $K_{\mu 2}$ and $K_{2\pi}$ events. In the muon sample all events with signal in the photon veto detectors are rejected. The efficiency is studied in bins of momentum due to the large variation of the RICH performances with respect to the pion momentum. The total muon and pion efficiencies are shown in figure 6. In the range of momentum [15, 35] GeV/c the muon efficiency is at the required level of 10^{-7} with a pion efficiency of around 60%.

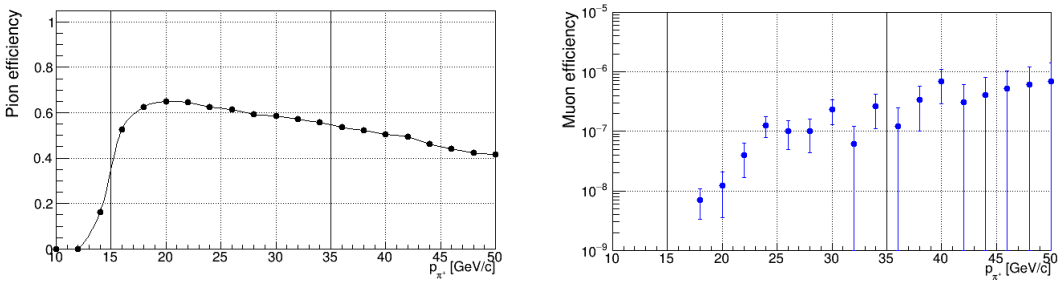

Figure 6. Particle identification performance for selected pions: on the left pion efficiency, on the right muon efficiency.

3.3 Photon Veto

The $K^+ \to \pi^+\pi^0$ decay is the second leading decay channel of charged kaons. The rejection of the kinematic and radiative tails of this process is fundamental for the $K^+ \to \pi^+\nu\bar{\nu}$ measurement. The main decay mode for neutral pions is in two photons ($BR(\pi^0 \to \gamma\gamma) = 98.8\%$ [10]). The requirement

of the track momentum in the region [15, 35] GeV/c results in π^0s with energies above 40 GeV and at least one of the photons in the final state is in the acceptance of a photon veto detector (LKr, LAVs, IRC or SAC).

The estimation of the π^0 rejection power requires large statistics of reconstructed $K^+ \to \pi^+\pi^0$ events, which is not achievable by using only the minimum-bias sample from the control trigger. A $K_{2\pi}$ selection based on the particle identification is therefore performed in parallel on Control and Physics trigger samples. The missing mass distribution of the selected events in the minimum-bias data is fitted with two concentric gaussians. The selected events in the physics trigger with signal in at least one of the photon veto detectors are rejected. The missing mass distribution is then fitted by the same two concentric gaussians with only the total amplitude left free in the fit. The π^0 inefficiency is then obtained by dividing the number of signal events in the physics and in the control samples. After correcting for the control trigger downscaling, the physics trigger efficiency and random losses, the π^0 inefficiency is determined as $(1.2 \pm 0.2) \times 10^{-7}$.

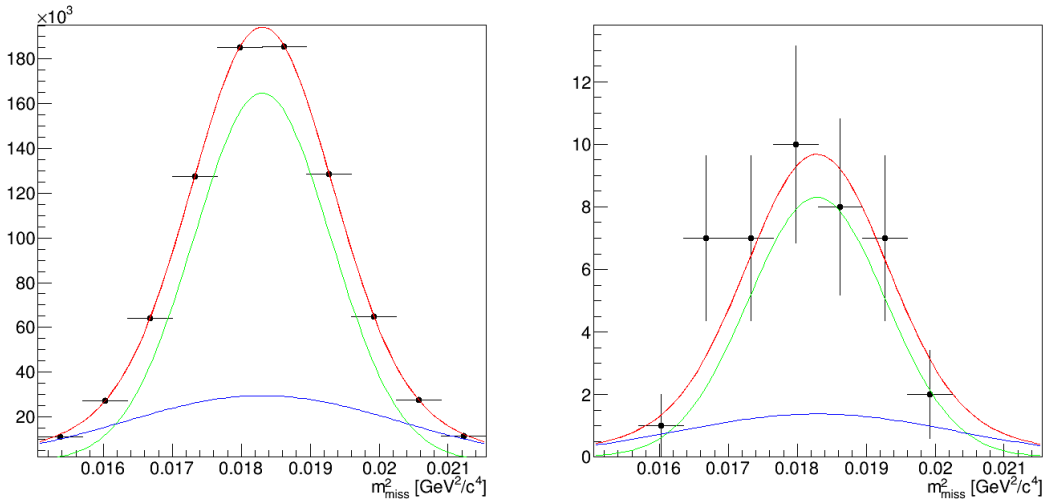

Figure 7. Fit of the $K^+ \to \pi^+\pi^0$ squared missing mass before (left) and after (right) applying the photon rejection for events selected respectively on the control and on the physics trigger sample.

4 Preliminary Results

The $K^+ \to \pi^+\pi^0$ decay, selected as described in 3.3, is chosen as normalisation channel, which allows a first order cancellation of systematic uncertainties due to the particle identification.

The analysis of 5% of the 2016 dataset allows to estimate the background contribution to the signal regions of the $K^+ \to \pi^+\nu\bar{\nu}$ decay. The signal expectation for 2.3×10^{10} kaon decays, the analysed fraction of collected data, is estimated to 0.064 SM events. Background contributions are estimated directly from events outside the signal regions and account for: 0.024, 0.011, 0.017 respectively from $K_{2\pi}$, $K_{\mu 2}$ and $K_{3\pi}$.

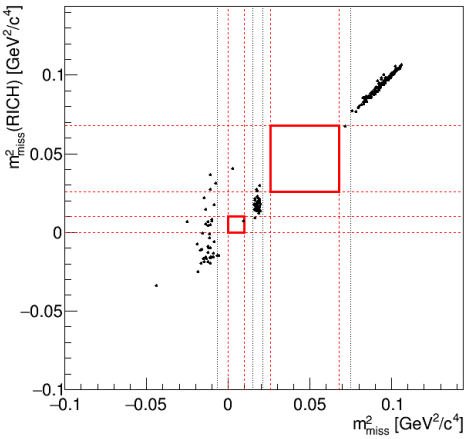

Figure 8. Missing Mass distribution, evaluated with GTK and RICH on the Y-axis and with GTK and Spectrometer on the X-axis, for full selection on 5% of 2016 dataset.

The final distribution of m^2_{miss}, computed with the GTK-RICH on the y-axis and with the GTK-STRAW on the x-axis, based on 2.3×10^{10} kaon decays is presented in figure 8. The only event appearing inside the signal region is rejected by the missing mass distribution computed with the nominal kaon momentum and the STRAW.

Refinement of the analysis to increase the signal acceptance and further improve background suppression is ongoing with the goal of reaching standard model sensitivity with the full 2016 data sample.

5 Conclusion and Outlook

The rare kaon decay $K^+ \to \pi^+\nu\bar{\nu}$ is one of the cleanest and most promising channel for the search of new physics. The NA62 experiment is running at CERN to reach 10% precision on the measurement of $BR(K^+ \to \pi^+\nu\bar{\nu})$. Preliminary results on a dataset containing 2.3×10^{10} kaon decays show that backgrounds are under control. No signal was observed inside the signal regions. The analysis of the complete 2016 data sample will reach the Standard Model sensitivity ($O(1)$ SM event expected).

The analysis of the data collected in 2017 and in the scheduled run of 2018 will allow to detect several tens of events, improving significantly the current branching ratio measurement. Extension of the data taking after 2018 to achieve 10% precision is currently under discussion.

References

[1] S. L. Glashow, J. Iliopoulos, and L. Maiani, Phys. Rev. D **2**, 1285 (1970)

[2] A. J. Buras, D. Buttazzo, J. Girrbach-Noe, and R. Knegjens, JHEP **1511**, 033 (2015)
[3] F. Mescia and C. Smith, Phys. Rev. D **76**, 034017 (2007)
[4] A. J. Buras, D. Buttazzo, J. Girrbach-Noe, and R. Knegjens, JHEP **1411**, 121 (2014)
[5] J.K. Ahn, *et al.* [E391a Collaboration], Phys. Rev. D **81**, 072004 (2010)
[6] A.V. Artamonov, *et al.* [E949 Collaboration], Phys. Rev. D **79**, 092004 (2009)
[7] T. Yamanaka [KOTO Collaboration], PTEP **2012**, 02B006 (2012)
[8] K. Shiomi, in proceedings of KAON 2016 conference, J. Phys. Conf. Ser. **800**, 012023 (2017)
[9] E. Cortina Gil, *et al.*, NA62 Collaboration, JINST **12** no.05, P05025 (2017)
[10] C. Patrignani, *et al.* (Particle Data Group), Chin. Phys. C **40**, 100001 (2016)